

## Adiabatic turbo spin echo for human applications at 7T.

I. M. van Kalleveen<sup>1</sup>, V. O. Boer<sup>1</sup>, P. Luijten<sup>1</sup>, J. J. Zwanenburg<sup>1</sup>, and D. W. Klomp<sup>1</sup>

<sup>1</sup>Radiology, UMC Utrecht, Utrecht, Netherlands

### Introduction

Non uniform  $B_1$  fields in high field clinical MRI can cause severe image artefacts when conventional RF pulses are used. This cancellation is due to the shortened wavelength and dielectric effects at high field. Particularly in MR sequences that encompass many RF pulses, e.g. turbo spin echo (TSE), complete signal cancellation may occur in certain areas. When using a surface coil, these problems become even more challenging, due to the spatial dependency of the  $B_1$  field. An alternative may be to apply adiabatic TSE sequences that are insensitive to  $B_1$  non uniformity, as was shown for the rat brain using surface coils<sup>[1]</sup>. Here we investigate the potential of using adiabatic TSE at 7T with surface coil transceivers in human applications. The adiabatic RF pulses were tuned to deal with the constraints in  $B_1$  strength and RF power deposition. As a consequence the phase coherence is compromised, as well as the dynamic range in  $B_1$ . Bloch simulations and phantom measurements are obtained to reveal these limitations. Using proper k-space sampling, we still demonstrate improved image quality of the adiabatic TSE versus the conventional TSE in the brain and the carotid artery.

### Methods

An adiabatic TSE<sup>[1]</sup> (Fig. 1) was implemented on a 7T whole body MR system (Philips, Cleveland, USA). A non selective adiabatic half passage (AHP)<sup>[2]</sup> of 2 ms (shape:tanh/tan) and a pair of slice selective adiabatic full passages (AFP)<sup>[2]</sup> of 10 ms each (shape:sech/tan) was used to obtain the first echo, while another up to 14 echoes were obtained with  $B_1$  independent plane rotation pulses (BIR4)<sup>[2]</sup> of 6 ms each (shape:tanh/tan). As the AFP's are used for slice selection, the bandwidth of the non-selective AHP and BIR4 can be small, enabling the use of low  $B_1$  values ( $\geq 15 \mu\text{T}$ ), and thereby depositing relatively low RF power in tissue. For all experiments, a transmit and receive surface coil (Machnet B.V., Eelde, The Netherlands) was used, consisting of two loops with a diameter of 5 cm each. Phantom measurements were obtained to optimize k-space sampling and to verify the dynamic range in  $B_1$  for effective use of the adiabatic TSE. Images of the primary visual cortex and the left carotid artery were obtained in a healthy volunteer to validate the adiabatic TSE for *in vivo* applications (resolution=0.5x0.5 mm, slice thickness=2 mm, turbo factor=7,  $T_R=2000$  ms,  $T_E=30$  ms,  $T_E'=15$  ms).

### Results

The even and odd BIR4 pulses result in phase alternations, as shown by Bloch simulations (Fig. 2). The effects of this phase alternation can be minimized by splitting up the even and odd echoes of the BIR4 in k-space (Fig. 3). When the strength of the transmit field is increased to three times the nominal value, artifacts are introduced in the image, as shown in simulations (Fig. 2) and phantom measurements (Fig. 3 versus Fig. 4). Still the adiabatic TSE provides better image quality than the conventional TSE (Fig. 4). Comparing *in vivo* data of the adiabatic TSE with the conventional TSE (Fig. 5 and 6), the adiabatic TSE does improve image quality.

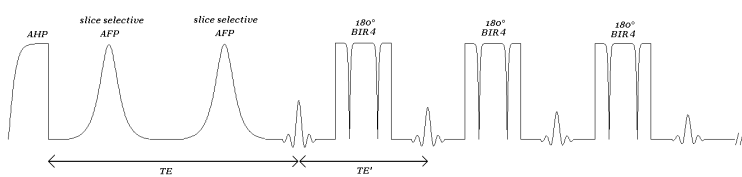


Fig. 1. Adiabatic TSE sequence

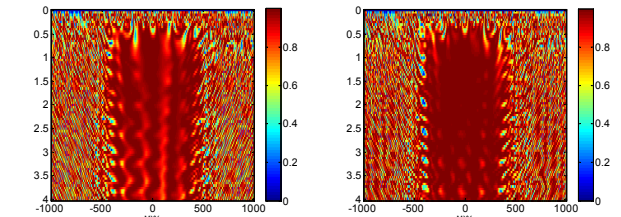


Fig. 2. Bloch simulations of adiabatic TSE pulses. The horizontal axis represents the offset frequency (Hz) and the vertical axis represents the  $B_1$  value (kHz). a) The magnetization after 3 BIR's and b) after 4 BIR's. Note that the 4<sup>th</sup> BIR4 corrects most of the phase errors that show up after the 3<sup>rd</sup> BIR4. Also notice that the adiabatic regime is limited.



Fig. 3. a) Conventional TSE, b) adiabatic TSE without splitting the even and odd echoes, and c) the adiabatic TSE where the even and odd echoes are separated in k-space.



Fig. 4. The same scans as Fig. 2, only with twice the  $B_1$ .

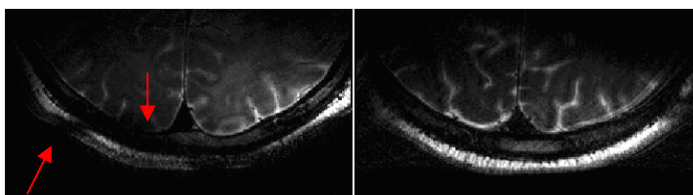


Fig. 5. A single slice of the primary visual cortex of a healthy volunteer. The left image is acquired with a conventional TSE. Note the black band through the skull. The right image was acquired with an adiabatic TSE. Note the absence of signal voids in the skull and brain structure.

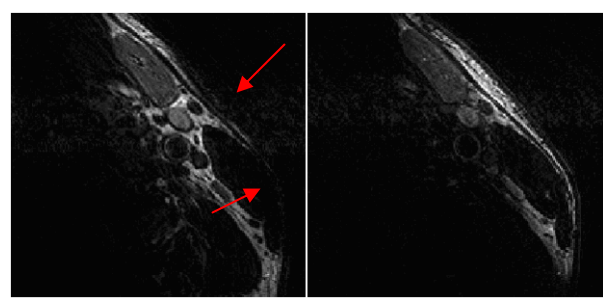


Fig. 6. A single slice of the left carotid artery of a healthy volunteer. The left image is acquired with a conventional TSE. Note the low intensity of the mandible. The right image was acquired with an adiabatic TSE. Note the uniform intensity of the mandible.

### Conclusion and discussion

In this work the limitations and potentials of adiabatic TSE have been demonstrated for human applications at 7T. To create adiabatic pulses for low and inhomogeneous  $B_1$  strengths and low SAR, the frequency sweep can be lowered. As a result, the adiabatic condition will be satisfied at lower  $B_1$  values, but at the expense of phase instability at three times the nominal  $B_1$ . Still, compared to the conventional TSE, the adiabatic TSE provides a much more homogeneous  $T_2$  weighted image without signal dropout.

### References

[1] De Graaf et al. NMR in Biomed 2003;16(29). [2] Garwood et al. Journal of Magnetic Resonance 2001;153(155).